Tuning and tailoring of broadband quantum-well infrared photodetector responsivity spectrum

S. V. Bandara, S. D. Gunapala, J. K. Liu, S. B. Rafol, C. J. Hill, D. Z.-Y. Ting, J. M. Mumolo, and T. Q. Trinh
Jet Propulsion Laboratory, California Institute of Technology 4800, Oak Grove Drive, Pasadena, California 91109

J. M. Fastenau and A. W. K. Liu
IQE, Inc., 119 Technology Drive, Bethlehem, Pennsylvania 18015

(Received 6 December 2004; accepted 10 March 2005; published online 6 April 2005)

The spectral response of quantum-well infrared photodetectors (QWIPs) based on the III-V material system are tailorable to narrow or broad bandwidths within mid- and long-wavelength infrared bands. Typical broad-band QWIPs show considerable spectral shape change with bias voltage, particularly near the cut-off wavelength region. Two alternatives to the typical broadband QWIP design have been demonstrated. These designs consist of two multiquantum-well (QW) stacks or alternatively placed QWs and produce nearly fixed spectrums within the operating bias voltages. Flexibility in many design parameters of these detectors allows for tuning and tailoring the spectral shape according to application requirements, specifically for spectral imaging instruments. © *2005 American Institute of Physics*. [DOI: 10.1063/1.1900313]

Infrared spectroscopy is a widely used technique in both ground and space-based remote sensing instruments to obtain critical scientific information as well as real time detection and identification of targets. High resolution imaging spectrometers or interferometers performing such investigations require small-pixel, large-format focal plane arrays (FPAs) with high uniformity and operability. The GaAs/AlGaAs-based quantum well infrared photodetectors (QWIP) technology is an excellent choice for the development of such FPAs.[1,2] This technology has shown remarkable success in advancing low-cost, highly uniform, high-operability, large-format FPAs due to its mature fabrication and processing techniques.[2–4] In addition, multiquantum well (MQW) parameters of the GaAs/$Al_xGa_{1-x}As$ based QWIPs can be varied over a range wide enough to enable light detection at any wavelength range from 6 to 20 μm[1,2] and beyond.[5] By adding a few monolayers of $In_yGa_{1-y}As$ during the GaAs QW growth, the short wavelength limit can be extended to 3 μm.[6]

In order to cover a wider spectral range, these instruments require FPAs sensitive in wider wavelength bands. However, the responsivity spectrum of a typical QWIP is inherently narrower because the photoexcitation occurs between energy levels localized within the QWs that are separated by thick barriers. Typically, the responsivity spectra of the *bound* and *quasibound* excited state QWIPs are much narrower ($\Delta\lambda/\lambda \sim 10\%$) than the *continuum* QWIPs ($\Delta\lambda/\lambda \sim 24\%$).[1,2] This is due to the fact that, when the excited state is placed in the continuum band above the barrier, the energy width associated with the state becomes wide. The spectral band width of these QWIPs can be further increased by replacing single QWs with small superlattice structures, several QWs separated by thin barriers, in the MQW structure.[7] Such a scheme creates an excited state miniband due to overlap of the excited state wave functions of the QWs. Energy band calculations shows that excited state energy level spreading depends sharply on the with of the superlattice barrier at smaller thicknesses. Following this technique, broadband QWIPs with spectral bandwidth up to $\Delta\lambda/\lambda \sim 50\%$ have been demonstrated.[7,8]

Unlike in narrow band QWIPs, broadband QWIPs show considerable spectral shape change with bias voltage, particularly near the cut-off wavelength region, as shown in Fig. 1. The actual device contains 35 periods of three-quantum-well superlattice separated by 600 Å $Al_{0.16}Ga_{0.84}As$ barriers. The well width and barrier thickness of the superlattice are 70 and 60 Å, respectively. The emitter and collector contact layers and QWs in the structure are doped with Si up to a carrier density of $n=2\times10^{17}$ cm^{-3}. The cause of this long cut-off shift can be attributed to the finite energy spreading of the excited state in the superlattice structure used in broadband QWIPs. The excited state energy levels associated with longer wavelengths are more strongly bound than those associated with shorter wavelengths. Therefore, it is required to apply a higher bias voltage to transport photoexcited electrons associated with longer wavelengths. The cause of this peak shift can be explained using the optical gain (g_p) which is defined by $R(\lambda)=(e/h\upsilon)\eta(\lambda)g_p(\lambda)$ where R is the responsivity, η is the absorption quantum efficiency, e is the elec-

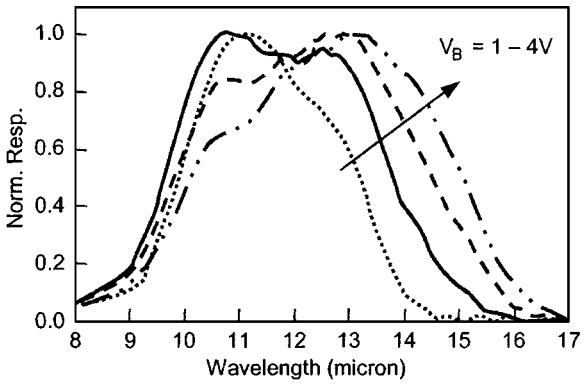

FIG. 1. Bias dependence spectral responsivity of a broadband QWIP structure which is created by replacing single-QWs in the narrow-band structure by few period superlattices.

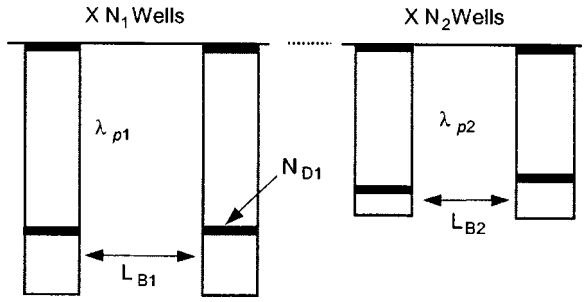

FIG. 2. Schematic conduction band diagram of a "stack design" broadband QWIP which consists of two stacks of MQW structures designed to respond at two different wavelengths (λ_{p1} and λ_{p2}) within the required broad wavelength band. N_1 and N_2, N_{D1} and N_{D2}, and L_{B1} and L_{B2} pairs represent different number of wells, well-doping densities, and barrier thickness in each MQW structure.

tronic charge, and hv is the photoexcitation energy.[1,7] For longer wavelengths, it is necessary to apply a higher bias voltage to obtain a reasonable nonzero value for g_p, while for shorter wavelengths g_p starts from zero bias. This can be attributed to the behavior of transmission probability factor (γ) in g_p, i.e. $g_p \propto \gamma$. The γ is smaller for low energy photoexcited electrons, i.e., longer wavelength transitions, because those electrons need to tunnel through a barrier to contribute to the photocurrent.

This change in spectral shape due to the bias voltage is an undesirable property for spectral imaging instruments because it could complicate the calibration process. If the spectral shape is fixed, the operating bias voltage of the FPA can be used as a parameter to optimize instrument performance during the imaging of different targets against different backgrounds. In order to accommodate this flexibility, we have considered two alternate designs for broadband QWIPs based on discrete narrow band QWIPs. Figure 2 shows a schematic conduction band diagram of the "stack design," which consists of two stacks of MQW structures designed to respond at two different wavelengths within the required broad wavelength band. A similar design scheme was used in the past for tunable multi-band QWIPs.[9,10] If the two MQW structures have dissimilar impedances, a disproportional bias voltage drop across the structures could lead to a dominant photocurrent response from a single structure. As the bias voltage changes, response could switch to the other structure, effectively acting as a voltage tunable detector.[9,10] Therefore, in order to keep the broadband spectral shape unchanged, it is essential to design two MQW structures with similar impedances, at least within the desired operating temperatures and bias voltages.

Table I shows three different structural parameters for "stack design" broadband QWIPs. Detector SB1 consists of two MQW structures, with similar barrier thickness and one designed for $\lambda p_1 = 6.8\ \mu$m and the other for $\lambda p_2 = 8.5\ \mu$m peak wavelength. Despite having a higher carrier density, the 6.8 μm QWIP has higher impedance than the 8.5 μm QWIP. Therefore, as the bias voltage increases, most of the bias drops across the 6.8 μm QWIP and then spreads over to the 8.5 μm QWIP. Figure 3(a) shows the spectral peak wavelength switching from $\lambda p_1 = 6.8\ \mu$m to $\lambda p_2 = 8.5\ \mu$m within a small bias voltage change (from $V_B = 3.5$ to 5.0 V) demonstrating the highly sensitive wavelength tunability of the device. Unlike detector SB1, SB2 and SB3 were designed to produce minimal spectral shape changes as bias voltage is varied. Detector SB2 comprises two MQW structures with $\lambda p_1 = 11.2\ \mu$m and $\lambda p_2 = 13.8\ \mu$m while detector SB3 comprises two MQW structures with $\lambda p_1 = 11.4\ \mu$m and $\lambda p_2 = 13.4\ \mu$m peak wavelengths. In order to reduce the impedance of the shorter wavelength MQWs to the level of the longer wavelength MQWs, bound-to-continuum QWs with thinner barriers were utilized, with the design parameters

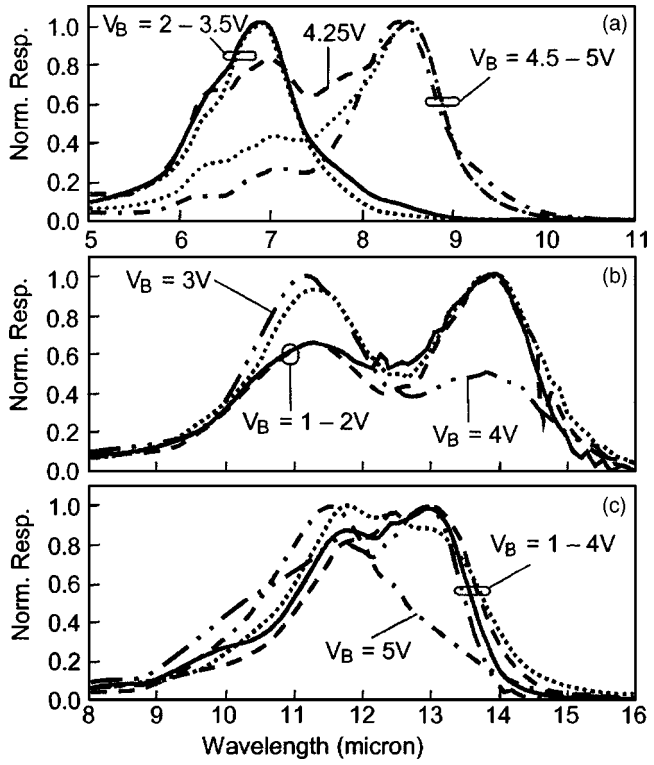

FIG. 3. Bias voltage dependence spectral responsivity of three different "stack design" QWIPs. (a) Due to unequal impedance of the two stacks, detector SB1 shows spectral tunability with the bias voltage. As shown in (b) and (c), SB2, and SB3 are designed to produce nearly unchanged spectra within the operating bias voltage range.

TABLE I. Design parameters of three different "stack design" broadband QWIPs.

	Detector SBI		Detector SB2		Detector SB3	
Design parameter	Stack 1	Stack 2	Stack 1	Stack 2	Stack 1	Stack 2
Peak $\lambda(\mu m)$	6.8	8.5	11.2	14.0	11.4	13.4
Number of wells	20	20	25	30	20	25
Well thickness (Å)	40(4% In)	48	56	75	59	70
Barrier thickness (Å)	300	300	400	500	400	500
Barrier Al%	28%	25%	19%	15%	18%	16%
Well doping (cm^{-3})	1.2×10^{18}	6×10^{17}	4×10^{17}	2×10^{17}	4×10^{17}	2×10^{17}

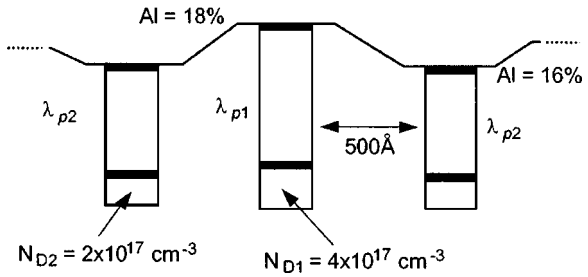

FIG. 4. Schematic conduction band diagram of the "intermix design" of a broadband QWIP consisting of multiple periods of alternatively placed, dissimilar QWs.

shown in Table I. The normalized spectral responsivity plots at different bias voltages in Fig. 3(b) shows nearly an unchanged broadband spectrum of SB2 within a 1–2 V voltage range, while Fig. 3(c) demonstrates the nearly unchanged broad-band spectrum of SB3 within a 1–3 V voltage range.

Figure 4 shows a schematic band diagram of an "intermix design" broadband QWIP consisting of multiple periods of alternatively placed dissimilar QWs designed to respond at $\lambda p_1 = 11.4\ \mu$m and $\lambda p_2 = 13.4\ \mu$m peak wavelengths. Each QW in the structure is separated by a 500 Å thick $Al_xGa_{1-x}As$ barrier with a bidirectionally graded Al composition of $x = 18$ to 16%. The impedances of both types of QWs were kept at similar values by utilizing a bound-continuum design with a higher doping density in shorter wavelength QWs. Figure 5 shows the normalized spectral

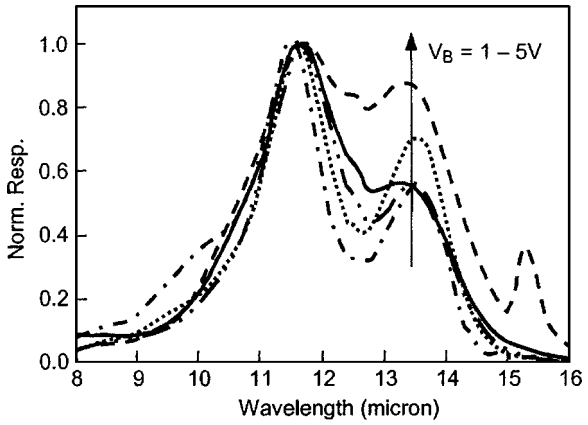

FIG. 5. Bias voltage dependence of the spectral responsivity of an "intermix design" broadband QWIP.

responsivity measured at different bias voltages. As designed, the broadband spectral shape is nearly unchanged within a $V_B = 1$–4 V bias range. The higher responsivity at shorter wavelengths ($\lambda p_1 = 11.4\ \mu$m) is attributed to the higher carrier density of the short wavelength QWs. One can obtain a smoother responsivity curve by properly adjusting the doping densities of the QWs or by adding more longer wavelength QWs to the MQW structure.

In summary, several methods for realizing broadband QWIP FPAs for spectral imaging instruments have been discussed. The requisite spectral band can be covered by utilizing a single broadband MQW or by stacking a few narrowband MQWs, thereby creating a multiband detector. It is important to avoid a change in spectral shape due to the bias voltage of the broadband FPAs utilized in spectral imaging instruments. Several alternatives to the typical broadband QWIP design have been demonstrated. A "stack design" which consists of two MQW stacks produces a nearly fixed spectrum as well as a highly tunable spectrum according to the impedance of each stack.

The research described in this article was carried out at the Jet Propulsion Laboratory, California Institute of Technology, and was partly sponsored by the National Aeronautics and Space Administration Offices of Aerospace Technology and Earth Sciences.

[1] B. F. Levine, J. Appl. Phys. **74**, R1 (1993).
[2] S. D. Gunapala and S. V. Bandara, *Quantum Well Infrared Photodetector (QWIP) Focal Plane Arrays*, *Semiconductors, and Semimetals*, Vol. 62, (Academic, New York, 1999), pp. 197–282.
[3] S. V. Bandara, S. D. Gunapala, F. M. Reininger, J. K. Liu, S. B. Rafol, J. M. Mumolo, D. Z. Ting, R. W. Chuang, T. Q. Trinh, J. M. Fastenau, and A. W. K. Liu, Proc. SPIE **5074**, 787 (2003).
[4] W. Cabanski, R. Breiter, R. Koch, K. H. Mauk, W. Rode, J. Ziegler, K. Eberhardt, R. Oelmaier, H. Schneider, and M. Walther, Proc. SPIE **4028**, 113 (2000).
[5] H. C. Liu, C. Y. Song, and A. J. Spring Thorpe, Appl. Phys. Lett. **84**, 4068 (2004).
[6] K. K. Choi, S. V. Bandara, S. D. Gunapala, W. K. Liu, and J. M. Fastenau, J. Appl. Phys. **91**, 5230 (2002).
[7] S. V. Bandara, S. D. Gunapala, J. K. Liu, E. M. Luong, J. M. Mumolo, W. Hong, D. K. Sengupta, and M. J. McKelvey, Appl. Phys. Lett. **72**, 2427 (1998).
[8] A. R. Ellis, A. Majumdar, K. K. Choi, J. L. Reno, and D. C. Tsui, Appl. Phys. Lett. **84**, 5127 (2004).
[9] H. C. Liu, J. Li, J. R. Thompson, Z. R. Wasilewski, M. Buchanan, and J. G. Simmons, IEEE Trans. Electron Devices **14**, 566 (1993).
[10] L. C. Lenchyshyn, H. C. Liu, M. Buchanan, and Z. R. Wasilewski, J. Appl. Phys. **79**, 8091 (1996).